

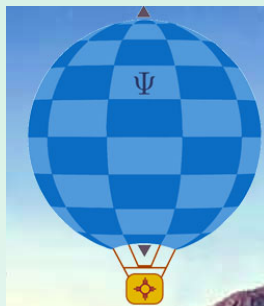
Reframing $SU(1,1)$ interferometry

- I. Introduction
- II. Itinerant signal, persistent modes
- III. Persistent signal, itinerant modes
 - a. *In situ* characterization of (lossy) pLONs for randomized boson sampling
 - b. Quantum illumination illuminated

Carlton M. Caves

Center for Quantum Information and Control, University of New Mexico

**C. M. Caves, “Reframing $SU(1,1)$ interferometry,
Advanced Quantum Technologies 3, 1900138 (2020),
[arXiv:1912.12530](https://arxiv.org/abs/1912.12530)**



CQuIC

Center for Quantum Information and Control



I. Introduction



**Oljeto Wash
Southern Utah**

SU(2) and SU(1,1) interferometry

B. Yurke, S. L. McCall, and J. R. Klauder, PRA **33**, 4033 (1986)

SU(2)

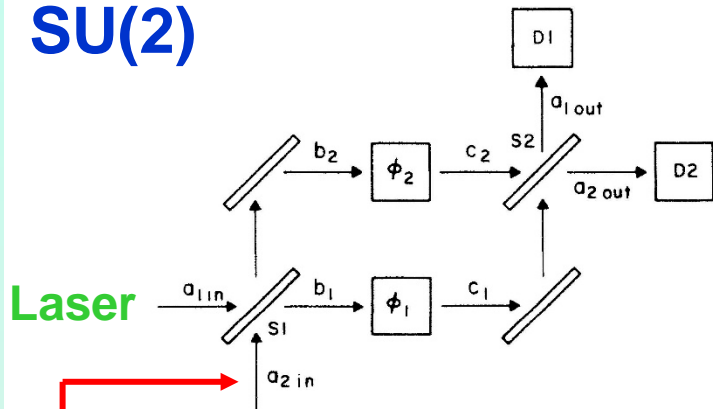


FIG. 1. A Mach-Zehnder interferometer. Light entering one of the two input ports a_{1in} or a_{2in} is split into two beams by beam splitter S1. The two light beams b_1 and b_2 accumulate a phase shift ϕ_1 and ϕ_2 , respectively, before entering beam splitter S2. The photons leaving the interferometer are counted by detectors D1 and D2.

To beat the quantum noise limit (QNL), put squeezed vacuum into the antisymmetric port.

Done in LIGO/Virgo O3.

Event rate up from about 1/month to 1/week.

SU(1,1)

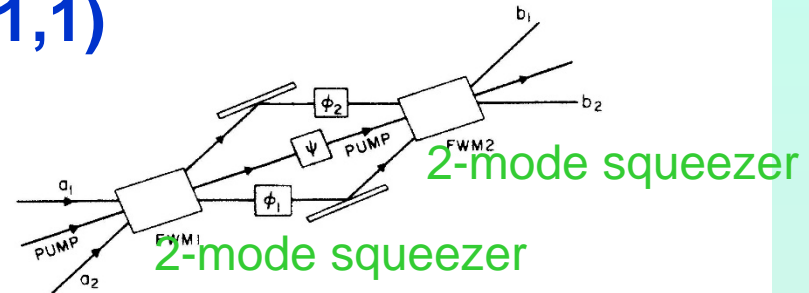


FIG. 6. An SU(1,1) interferometer. The beam splitters of a conventional interferometer have been replaced by the four-wave mixers FWM1 and FWM2. The light pumping FWM2 is phase shifted from the light pumping FWM1 by the angle ψ .

LIGO: M. Tse *et al.*, PRL **123**, 231107 (2019).

Virgo: F. Acernese *et al.*, PRL **123**, 231108 (2019).

SU(2) and SU(1,1) interferometry

B. Yurke, S. L. McCall, and J. R. Klauder, PRA **33**, 4033 (1986)

Experiments:

J. Jing, C. Liu, Z. Zhou, Z. Y. Ou, and W. Zhang, Appl Phys Lett **99**, 011110 (2011). Optical

F. Hudelist, J. Kong, C. Liu, J. Jing, Z. Y. Ou, and W. Zhang, Nat Comm **5**, 3049 (2014). Optical

B. Chen, C. Qiu, S. Chen, J. Guo, L. Q. Chen, Z. Y. Ou, and W. Zhang, PRL **115**, 043602 (2015). Atom-light hybrid

C. Linnemann, H. Strobel, W. Muessel, J. Schulz, R. J. Lewis-Swan, K. V. Kheruntsyan, and M. K. Oberthaler, PRL **117**, 013001 (2016). BEC

B. E. Anderson, P. Gupta, B. L. Schmittberger, T. Horrom, C. Hermann-Avigliano, K. M. Jones, and P. D. Lett, PRA **95**, 063843 (2017). Truncated optical

B. E. Anderson, P. Gupta, B. L. Schmittberger, T. Horrom, C. Hermann-Avigliano, K. M. Jones, and P. D. Lett, Optica **4**, 752 (2017). Truncated optical

M. Manceau, G. Leuchs, F. Khalili, and M. Chekhova, PRL **119**, 223604 (2017).

J. Li, Y. Liu, N. Huo, S. M. Assed, X. Li, and Z. Y. Ou, PRA **97**, 052127 (2018). Optical

P. Gupta, B. L. Schmittberger, B. E. Anderson, K. M. Jones, and P. D. Lett, Opt Exp **26**, 291 (2018). Truncated optical

S. Liu, Y. Lou, J. Xin, J. Jing, PR Applied **10**, 064046 (2018). Optical

Y. Liu, N. Huo, J. Li, L. Cui, X. Li, and Z. J. Ou, Opt Exp **27**, 011292 (2019). Optical

G. Frascella, E. E. Mikhailov, N. Takanashi, R. V. Zakharov, O. V. Tikhonova, and M. V. Chekhova, Optica **6**, 1233 (2019). Optical

SU(1,1)

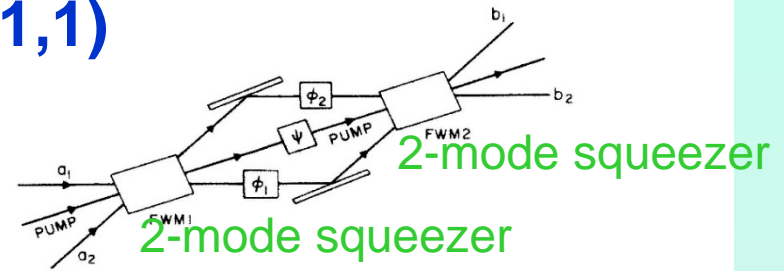


FIG. 6. An SU(1,1) interferometer. The beam splitters of a conventional interferometer have been replaced by the four-wave mixers FWM1 and FWM2. The light pumping FWM2 is phase shifted from the light pumping FWM1 by the angle ψ .

Let's reframe this as linear force detection.

Persistent signal, itinerant probe oscillators (modes) (Part II)

vs.

Itinerant signal, persistent probe oscillators, examined repeatedly with QND or back-action-evading (BAE) measurements (Part I)

II. Itinerant signal, persistent modes



Holstrandir Peninsula overlooking Ísafjarðardjúp
Westfjords, Iceland

Measuring one force quadrature:

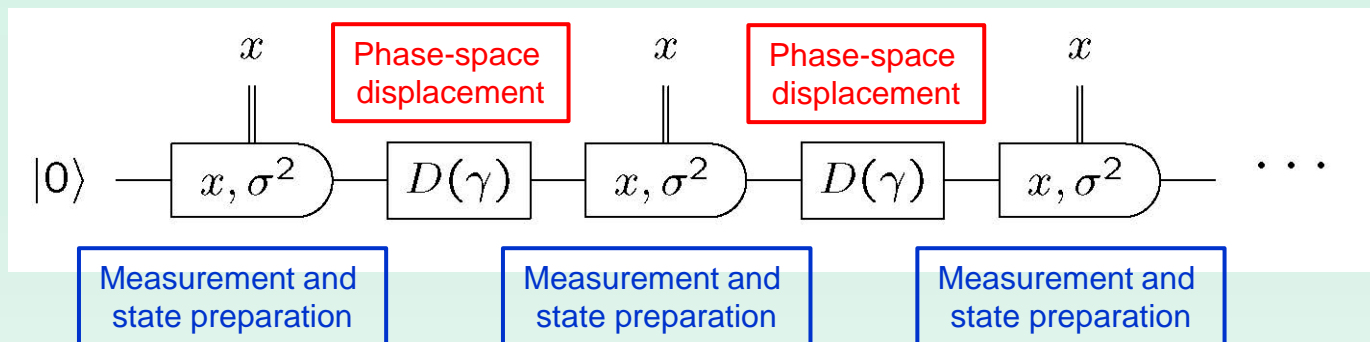
BAE (homodyne) measurements of quadrature component

1. Gravitational-wave tidal force on a metal-bar oscillator
2. Force on an opto-mechanical mode
3. Axion force on mode of a microwave resonator

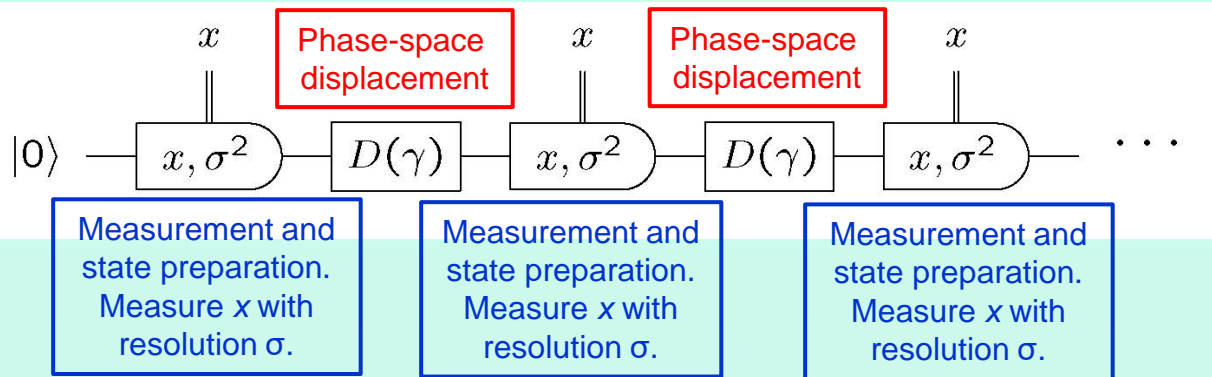
Force *displaces* the mode's complex amplitude.
Repeated measurements dominate the mode's coupling to the external world (e.g., dissipation).

$$\text{Mode } \hat{a} = \frac{1}{\sqrt{2}}(\hat{x} + i\hat{p})$$

\hat{a} , \hat{x} , and \hat{p} are constants in the rotating frame:
 \hat{a} is the phase-space *complex amplitude*; $\hat{x} = \hat{x}_1$
and $\hat{p} = \hat{x}_2$ are called *quadrature components*.



Measuring one force quadrature: BAE (homodyne) measurements of quadrature component



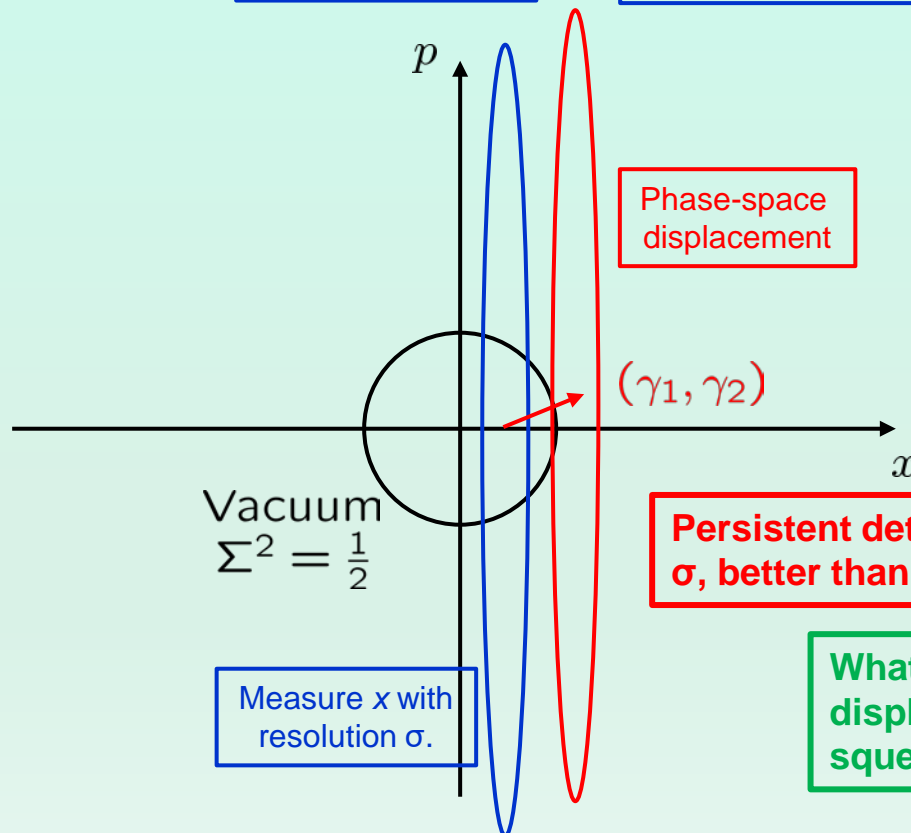
Displacement operator

$$D(\gamma) = e^{\gamma \hat{a}^\dagger - \gamma^* \hat{a}} = e^{i(\gamma_2 \hat{x} - \gamma_1 \hat{p})}$$

$$\gamma = (\gamma_1 + i\gamma_2)/\sqrt{2}$$

BAE Homodyne POVM with resolution σ^2

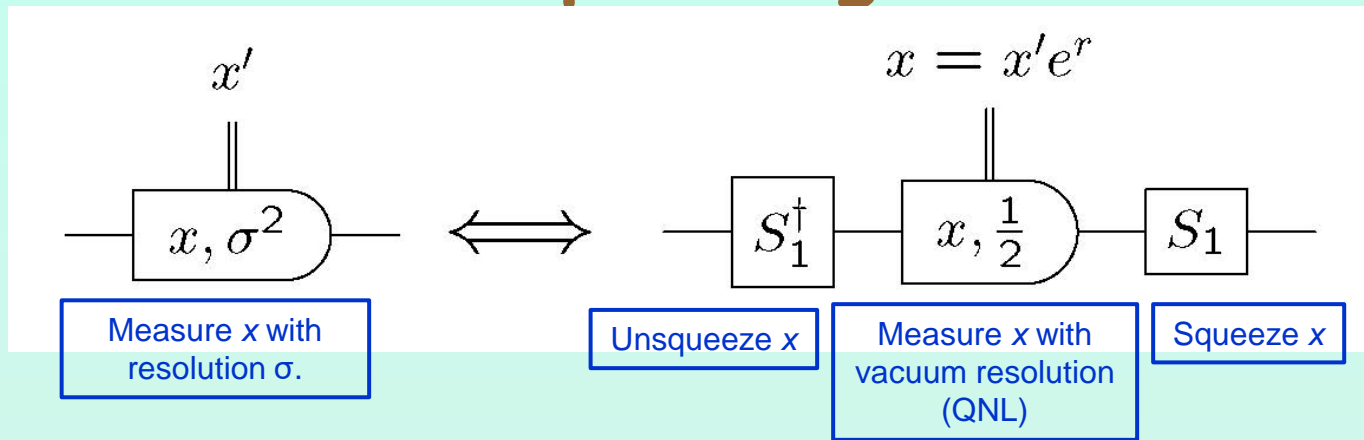
$$E_x^{\sigma^2} = \int dy \frac{e^{-(y-x)^2/2\sigma^2}}{\sqrt{2\pi\sigma^2}} |y\rangle\langle y|$$



Persistent detection of x displacement with resolution σ , better than the quantum-noise limit (QNL).

What about measurement of displaced squeezed states, i.e., squeezed heterodyne measurement?

Measuring one displacement quadrature: Squeezing



Single-mode squeeze operator

$$S_1 = e^{r(\hat{a}^2 - \hat{a}^{\dagger 2})/2} = e^{ir(\hat{x}\hat{p} + \hat{p}\hat{x})/2}$$

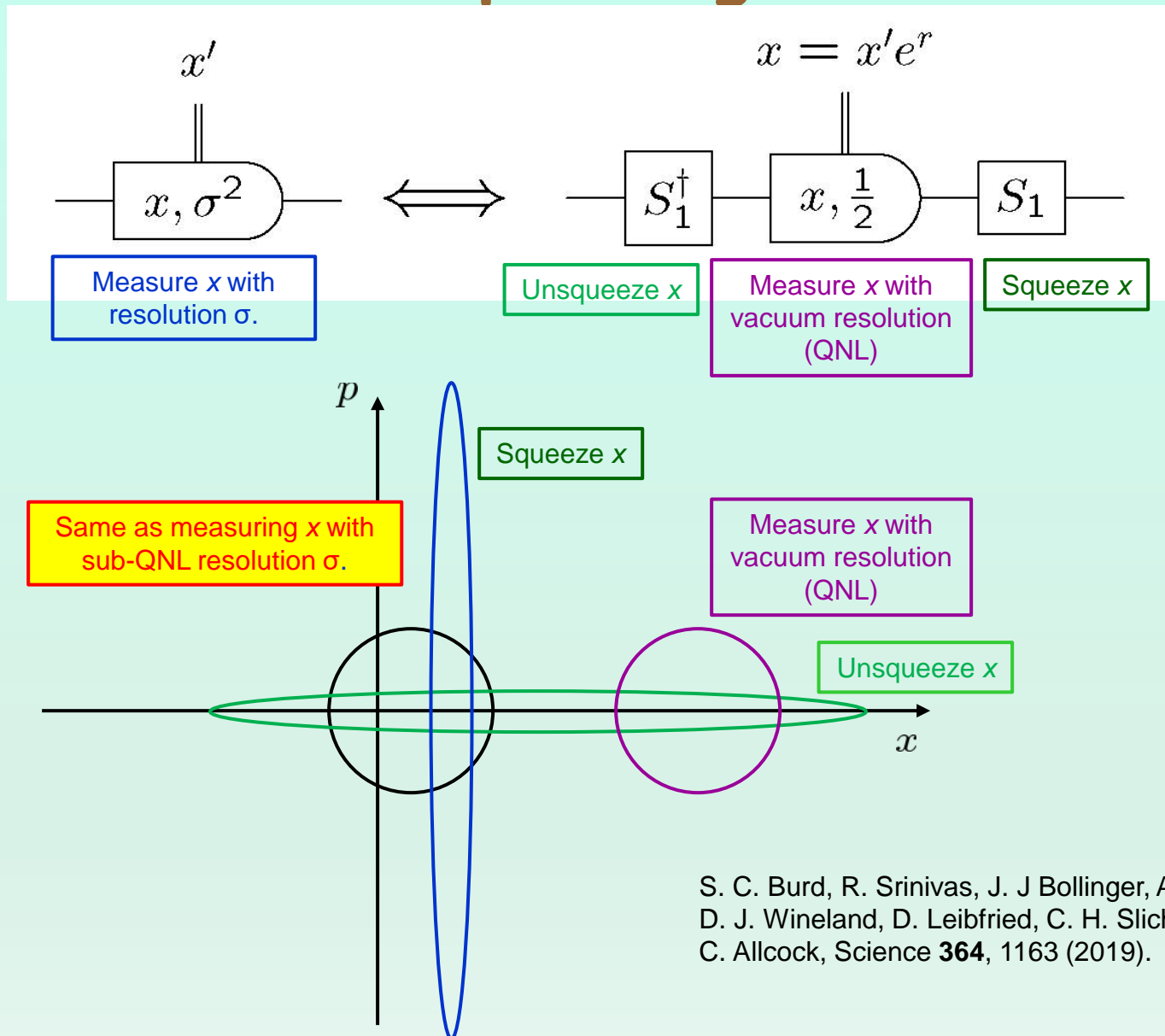
$$\sigma^2 = \frac{1}{2}e^{-2r}$$

$$S_1|y\rangle = e^{-r/2}|ye^{-r}\rangle$$

$$S_1^\dagger \hat{x} S_1 = \hat{x}e^{-r} \quad S_1^\dagger \hat{p} S_1 = \hat{p}e^r$$

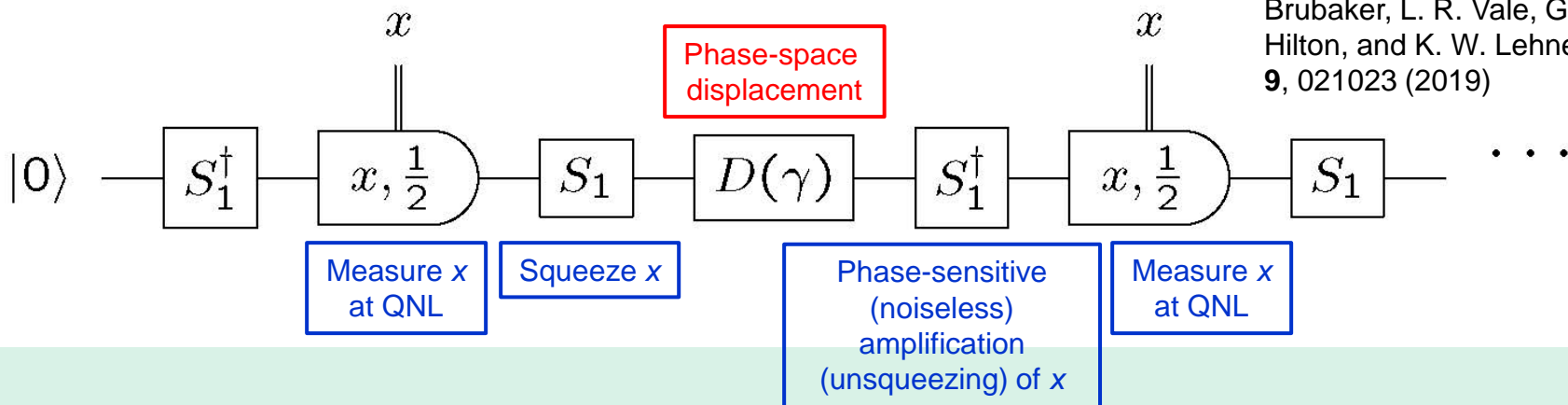
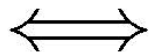
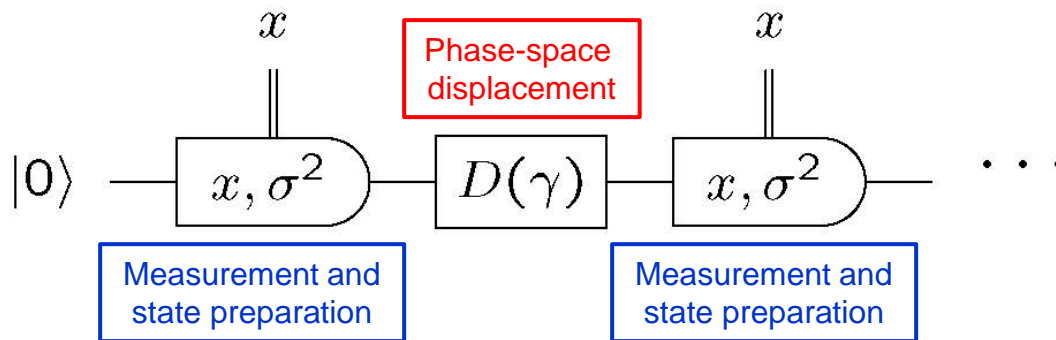
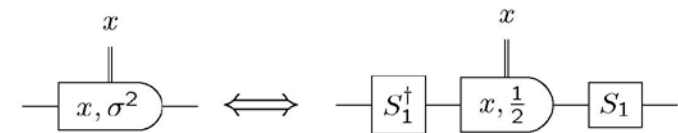
$$\begin{aligned} S_1 dx E_x^{1/2} S_1^\dagger &= dx \int dy \frac{e^{-(y-x)^2}}{\sqrt{\pi}} S_1|y\rangle \langle y| S_1^\dagger \\ &= dx \int d(ye^{-r}) \frac{e^{-(y-x)^2}}{\sqrt{\pi}} |ye^{-r}\rangle \langle ye^{-r}| \\ &= d(xe^{-r}) \int dy \frac{e^{-(y-xe^{-r})^2/2\sigma^2}}{\sqrt{2\pi\sigma^2}} |y\rangle \langle y| \\ &= dx' E_{x'}^{\sigma^2}, \quad x' = xe^{-r} \end{aligned}$$

Measuring one displacement quadrature: Squeezing



S. C. Burd, R. Srinivas, J. J. Bollinger, A. C. Wilson,
 D. J. Wineland, D. Leibfried, C. H. Slichter, and D. T.
 C. Allcock, *Science* **364**, 1163 (2019).

Measuring one displacement quadrature: Squeezing

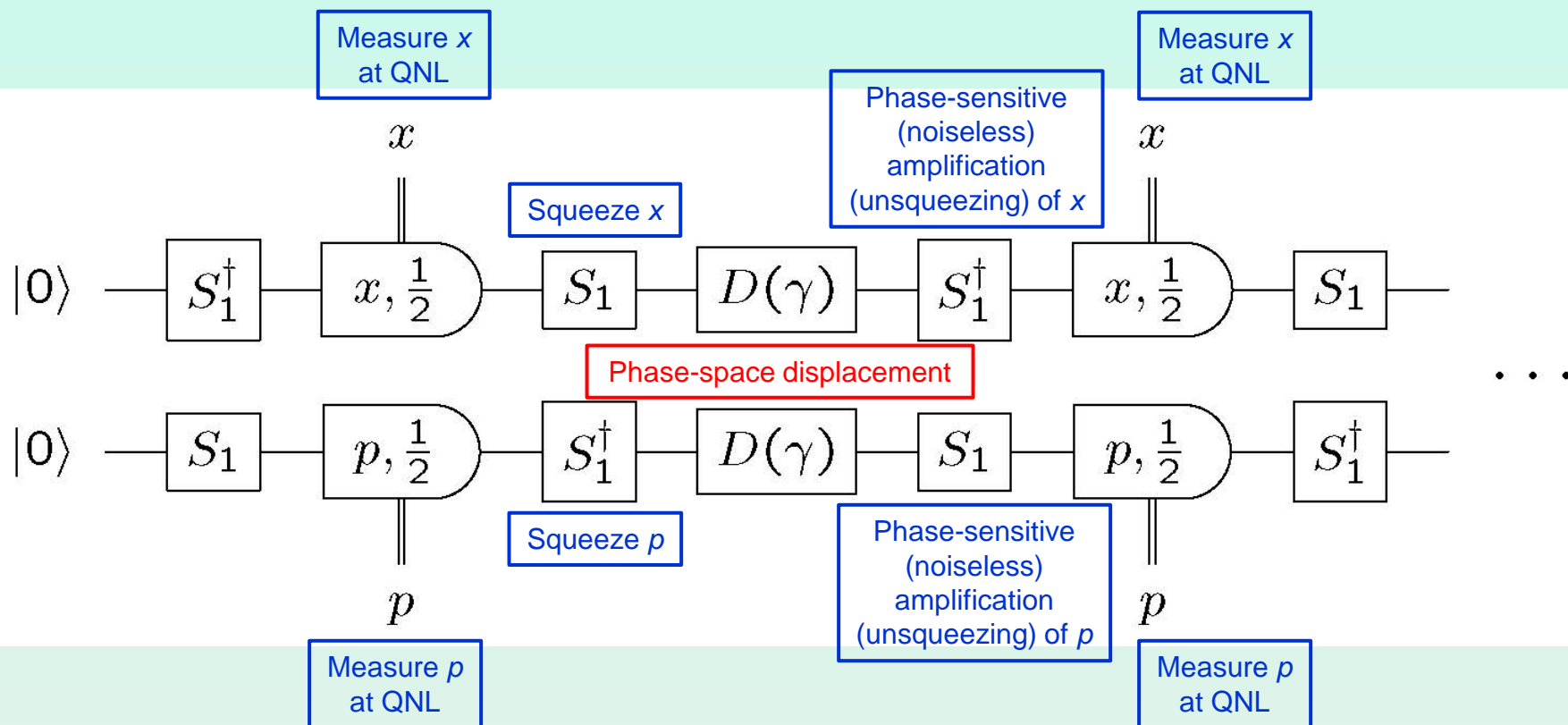


M. Malnou, D. A. Palken, B. M. Brubaker, L. R. Vale, G. C. Hilton, and K. W. Lehnert, PRX **9**, 021023 (2019)

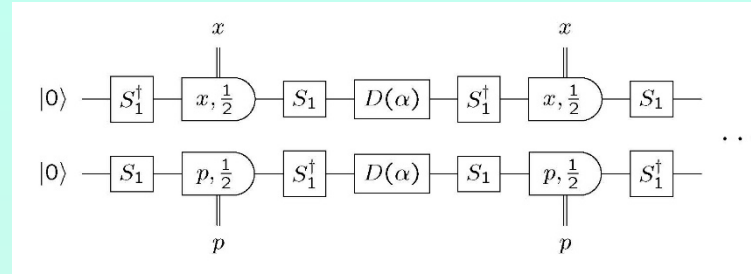
$$\begin{aligned}
 \hat{x} &\xrightarrow{\text{squeeze}} \hat{x}e^{-r} \xrightarrow{\text{displace}} \hat{x}e^{-r} + \gamma_1 \xrightarrow{\text{unsqueeze}} \hat{x} + \gamma_1 e^r \\
 \hat{p} &\xrightarrow{\text{unsqueeze}} \hat{p}e^r \xrightarrow{\text{displace}} \hat{p}e^r + \gamma_2 \xrightarrow{\text{squeeze}} \hat{p} + \gamma_2 e^{-r}
 \end{aligned}$$

Measuring both displacement quadratures: Squeezing

Couple two oscillators to the same force (could be tricky, depending on circumstances, but not hard in axion detection). Measure x on one and p on the other.



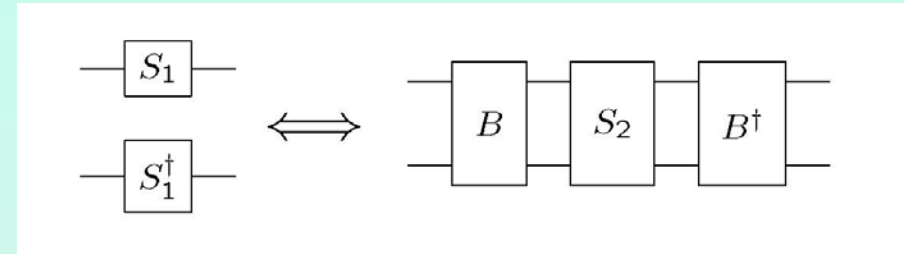
Measuring both displacement quadratures: $SU(1,1)$



Two-mode squeeze operator

$$S_2 = e^{r(\hat{a}\hat{b} - \hat{a}^\dagger\hat{b}^\dagger)}$$

$$B^\dagger S_2 B = S_1 \otimes S_1^\dagger$$

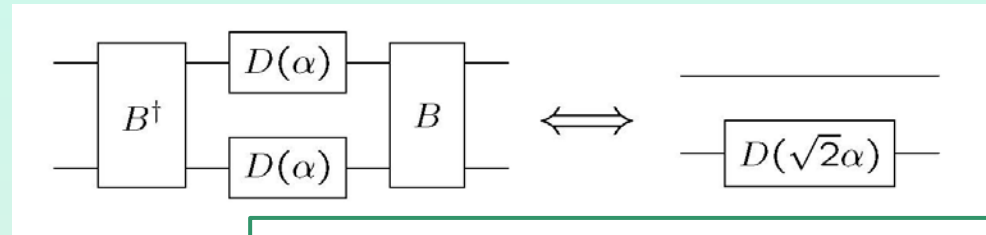


50-50 beamsplitter

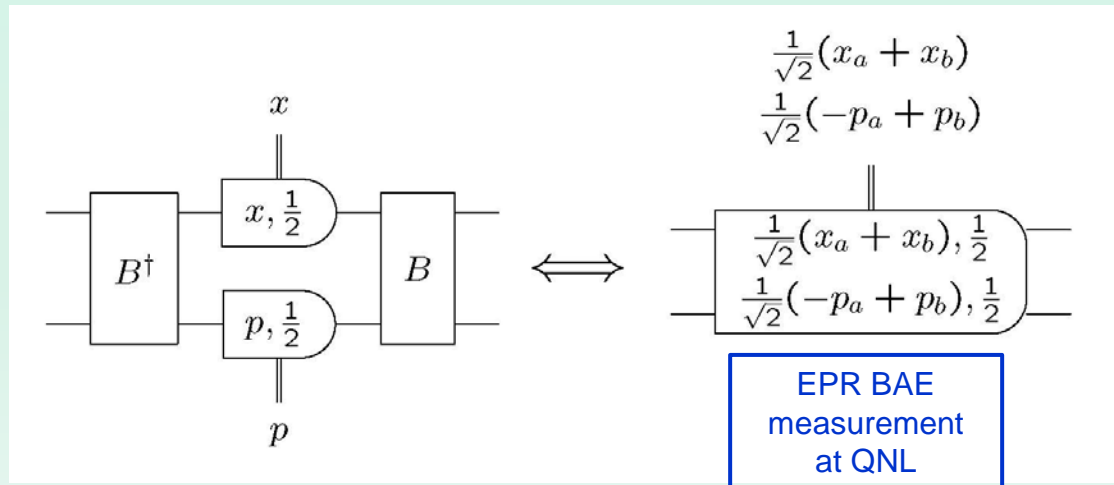
$$B = e^{(\hat{a}\hat{b}^\dagger - \hat{a}^\dagger\hat{b})\pi/4}$$

$$B^\dagger \hat{a} B = \frac{1}{\sqrt{2}}(\hat{a} - \hat{b})$$

$$B^\dagger \hat{b} B = \frac{1}{\sqrt{2}}(\hat{a} + \hat{b})$$

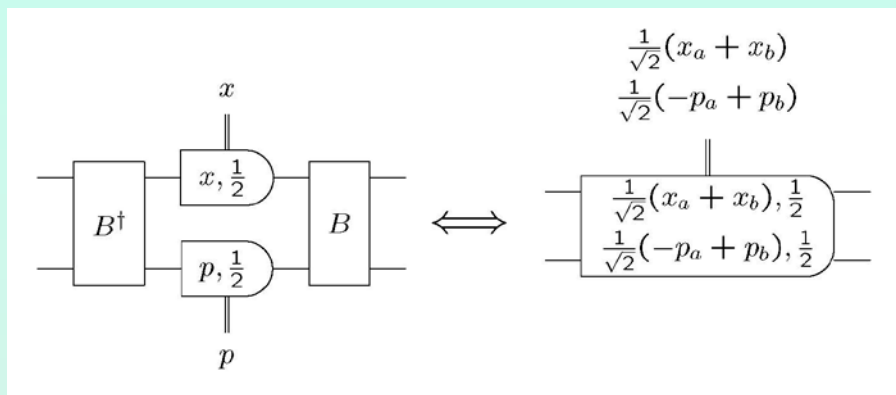
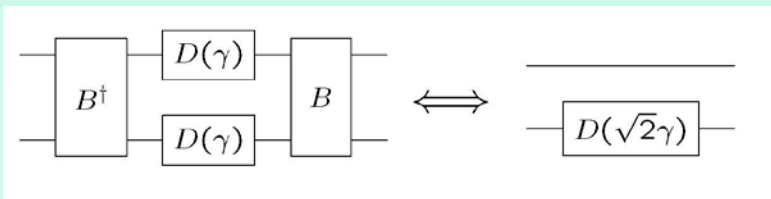
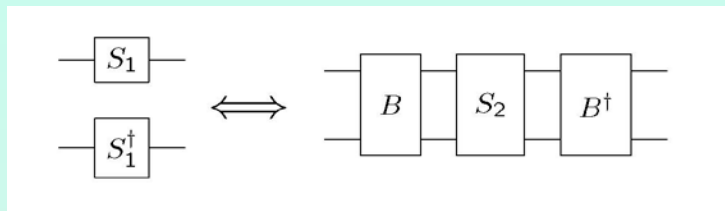
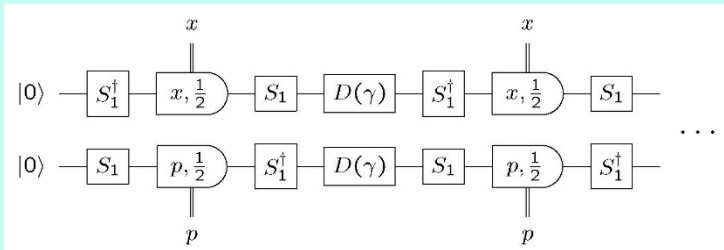


Phase-space displacement on only one oscillator



EPR BAE measurement at QNL

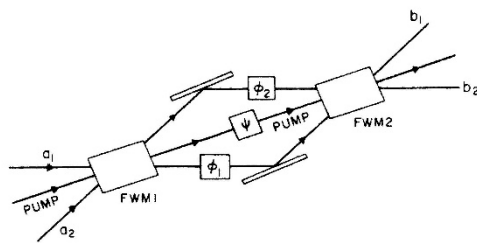
Measuring both displacement quadratures: $SU(1,1)$



H. Zheng, M. Silveri, R. T. Brierley, S. M. Girvin, and K. W. Lehnert, arXiv:1607.02529 [hep-ph]

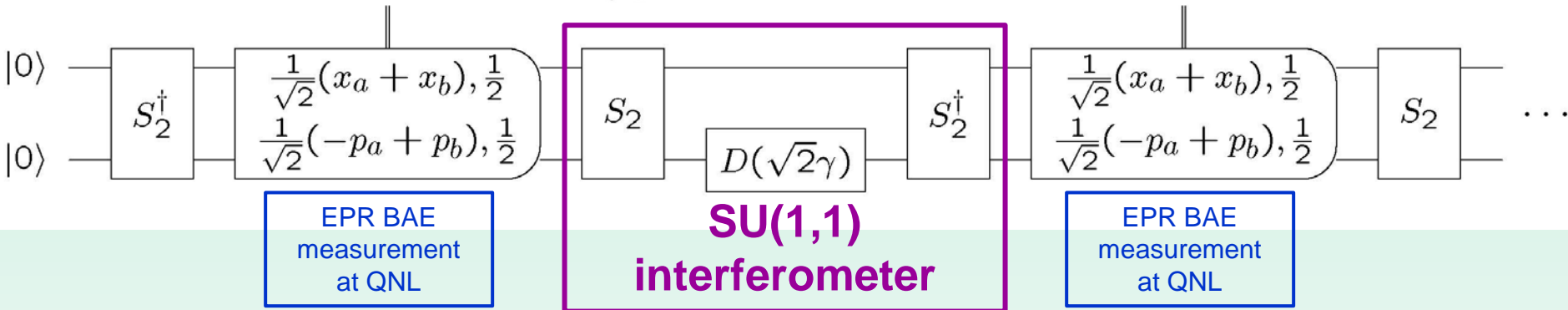
$$\frac{1}{\sqrt{2}}(x_a + x_b)$$

$$\frac{1}{\sqrt{2}}(-p_a + p_b)$$

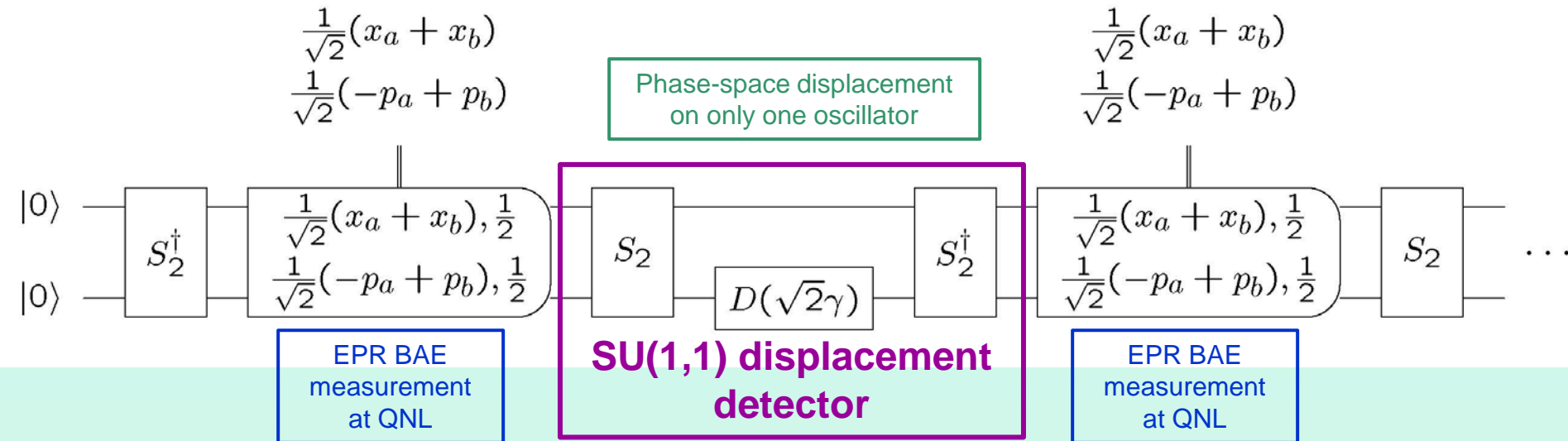


$$\frac{1}{\sqrt{2}}(x_a + x_b)$$

$$\frac{1}{\sqrt{2}}(-p_a + p_b)$$



Measuring both displacement quadratures



The EPR variables $(x_a + x_b)/\sqrt{2}$ and $(-p_a + p_b)/\sqrt{2}$ are squeezed, displaced, and then unsqueezed, providing displacement sensitivity beyond the QNL.

1. An interferometer uses interference at the final beamsplitter to transform phase shifts in the arms into amplitude signals that can be measured by square-law detection.
2. SU(1,1) interferometry works quite differently and isn't an interferometer at all. It is profitably reframed as a *displacement detector*, making BAE measurements of both quadrature displacements, using squeezing (noiseless deamplification) and unsqueezing (noiseless amplification) to achieve displacement sensitivity below the QNL, even though the measurements of quadrature components are not sub-QNL.

Measuring both displacement quadratures

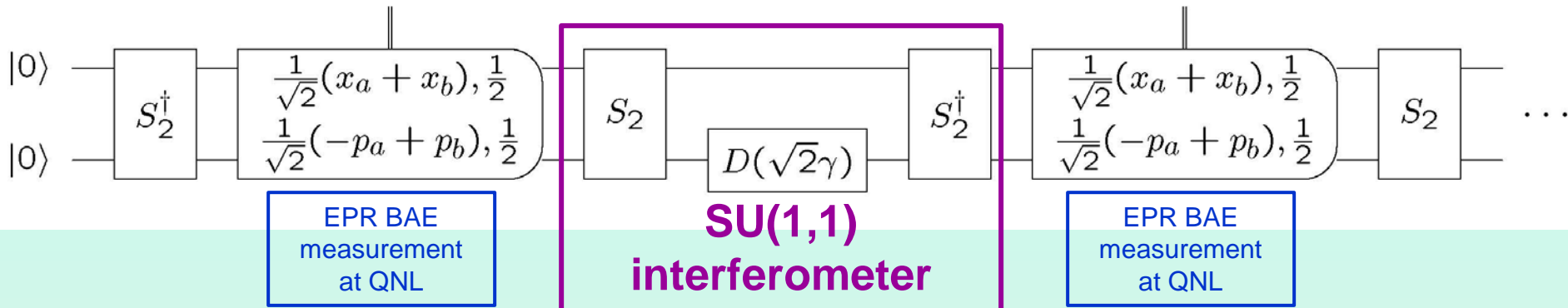
Squeezing version

$$\frac{1}{\sqrt{2}}(x_a + x_b)$$

$$\frac{1}{\sqrt{2}}(-p_a + p_b)$$

$$\frac{1}{\sqrt{2}}(x_a + x_b)$$

$$\frac{1}{\sqrt{2}}(-p_a + p_b)$$



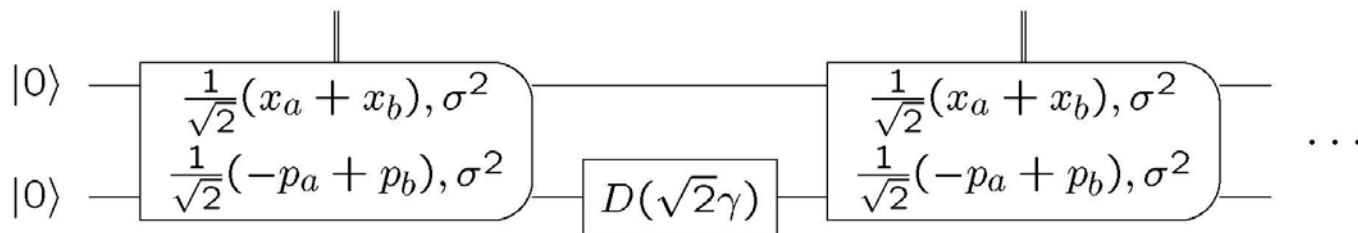
Measurement-based version

$$\frac{1}{\sqrt{2}}(x_a + x_b)$$

$$\frac{1}{\sqrt{2}}(-p_a + p_b)$$

$$\frac{1}{\sqrt{2}}(x_a + x_b)$$

$$\frac{1}{\sqrt{2}}(-p_a + p_b)$$



The EPR BAE variables $(\hat{x}_a + \hat{x}_b)/\sqrt{2}$ and $(-\hat{p}_a + \hat{p}_b)/\sqrt{2}$ are measured repeatedly on a pair of oscillators with resolution better than the SNL.

Reframing $SU(1,1)$

1. An interferometer uses interference at the final beamsplitter to transform phase shifts in the arms into amplitude signals that can be measured by square-law detection.
2. $SU(1,1)$ interferometry works quite differently and isn't an interferometer at all. It is profitably reframed as a *displacement detector*, making BAE measurements of both quadrature displacements, using squeezing (noiseless deamplification) and unsqueezing (noiseless amplification) to achieve displacement sensitivity below the QNL, even though the measurements of quadrature components are not sub-QNL.

Why is reframing important?

Thinking of $SU(1,1)$ as an interferometer that detects phase changes leads to the wrong questions, such as thinking about the Heisenberg limit.

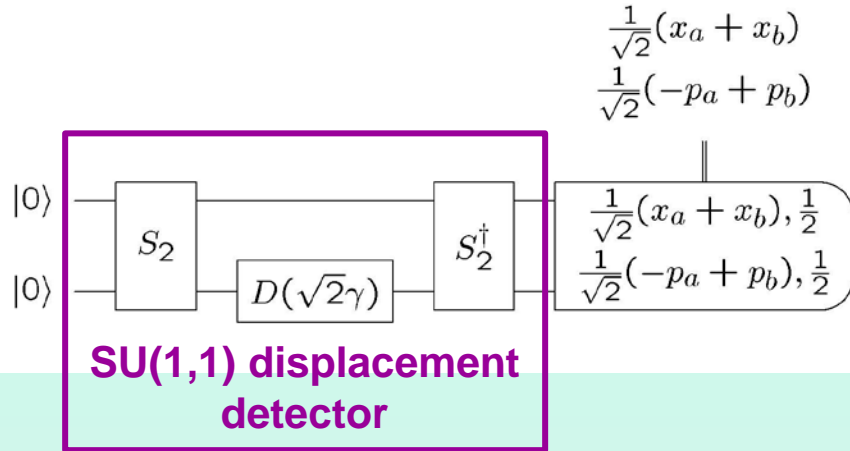
Reframing as a displacement detector focuses attention on the right questions: How much squeezing is available for noiseless amplification and de-amplification? How does one devise schemes that detect both displacement quadratures?



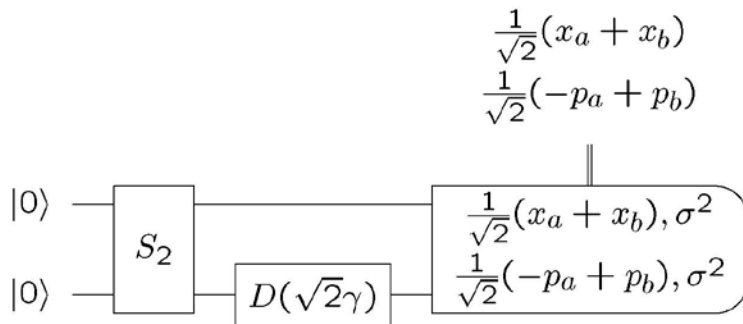
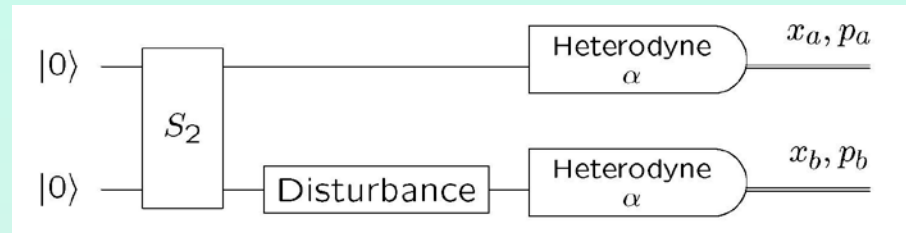
III. Persistent signal, itinerant modes

Dettifoss, Iceland

Persistent signal, itinerant modes

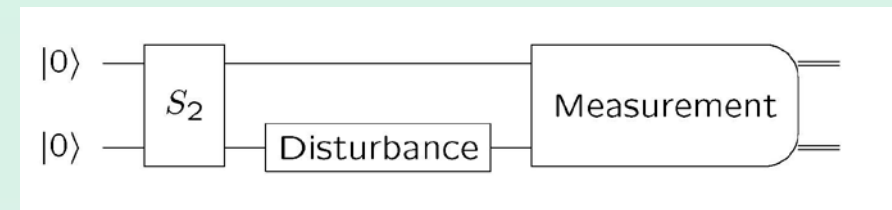


Interested in detecting a disturbance in mode b in repeated trials? Can use weak squeezing and measure all four quadrature components with heterodyne.



Truncated SU(1,1): omit second two-mode squeezer, and measure EPR quadratures at resolution σ .

Or, more generally, use the correlations of two-mode squeezed states to sense a disturbance on one of the modes.



III.a *In situ*
characterization of (lossy)
pLONs for randomized
boson sampling

Red-backed fairy wren
Oxley Common, Brisbane



Variegated fairy wren
Oxley Common, Brisbane

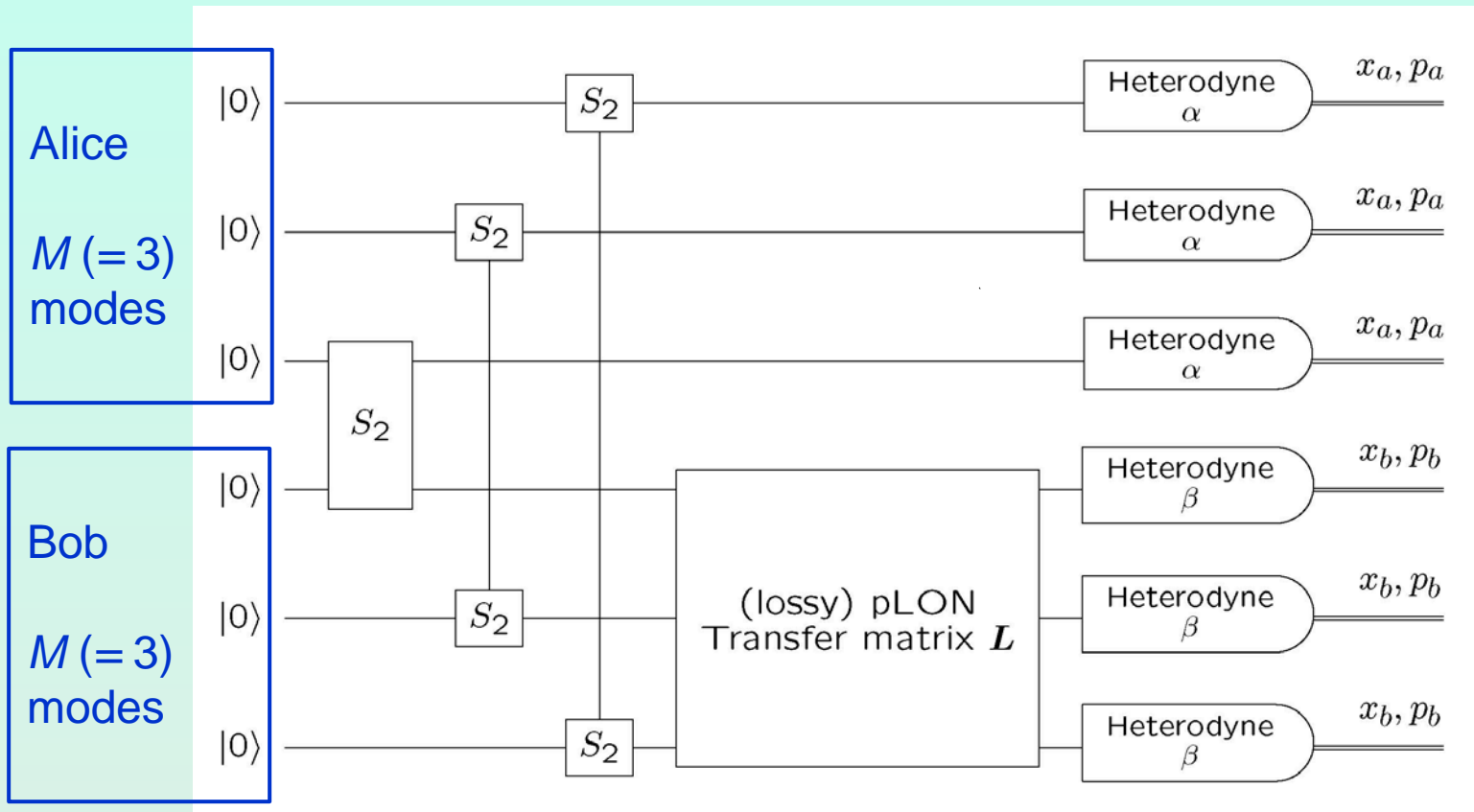


Western diamondback rattlesnake
My front yard, Sandia Heights



Characterization of pLON

Mean number of photons counted by Alice and into Bob's inputs is $N = M \sinh^2 r \simeq \sqrt{M}$ (birthday avoidance).

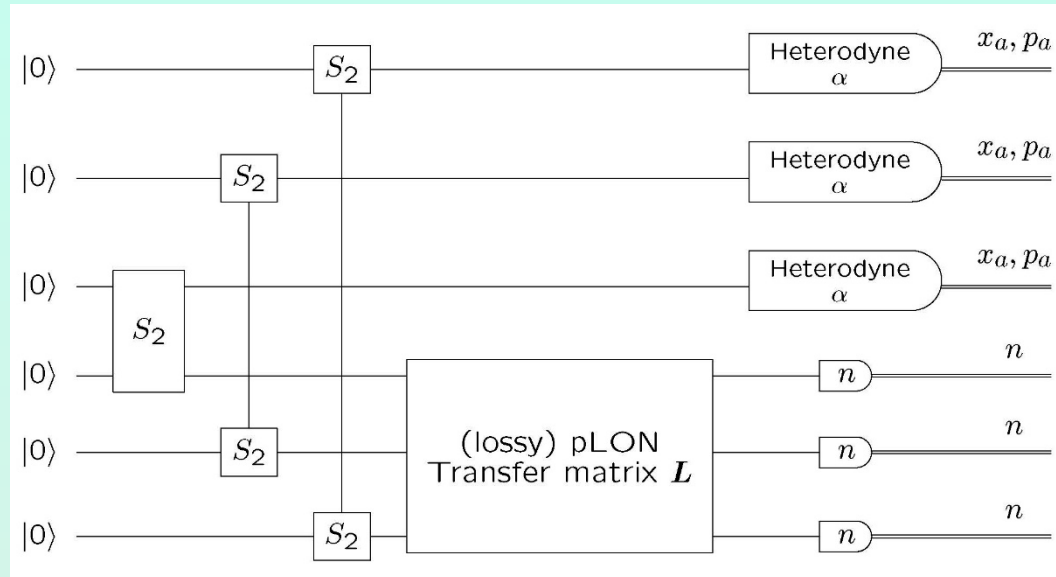


Given Alice's heterodyne outcomes α , which are drawn from thermal distributions, the input to Bob's pLON is the coherent state $|-\alpha \tanh r\rangle$; the output of Bob's pLON is $|-\alpha L \tanh r\rangle$.

If Bob's heterodyne outcome for mode i is 0, then $0 = \alpha L_i$ (statistically), with L_i being the i th column of the transfer matrix. The second moments of Alice's heterodyne outcomes for this case determine L_i .

In situ characterization and randomized boson sampling

S. Rahimi-Keshari, S. Baghbanzadeh, and C. M. Caves, Physical Review A **101**, 043809 (2020),



Characterization runs

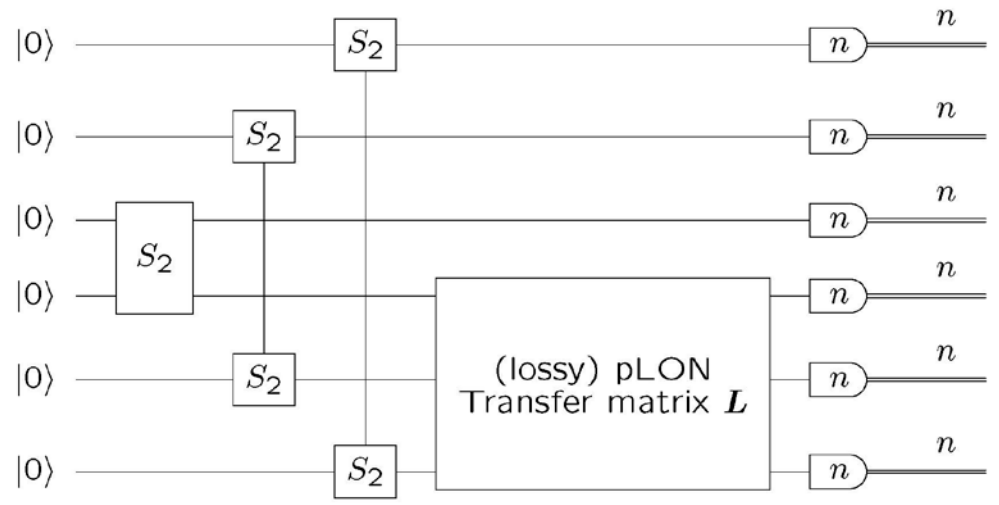
The second moments of Alice's heterodyne outcomes, conditioned on Bob's receiving vacuum in mode i , determine L_i .

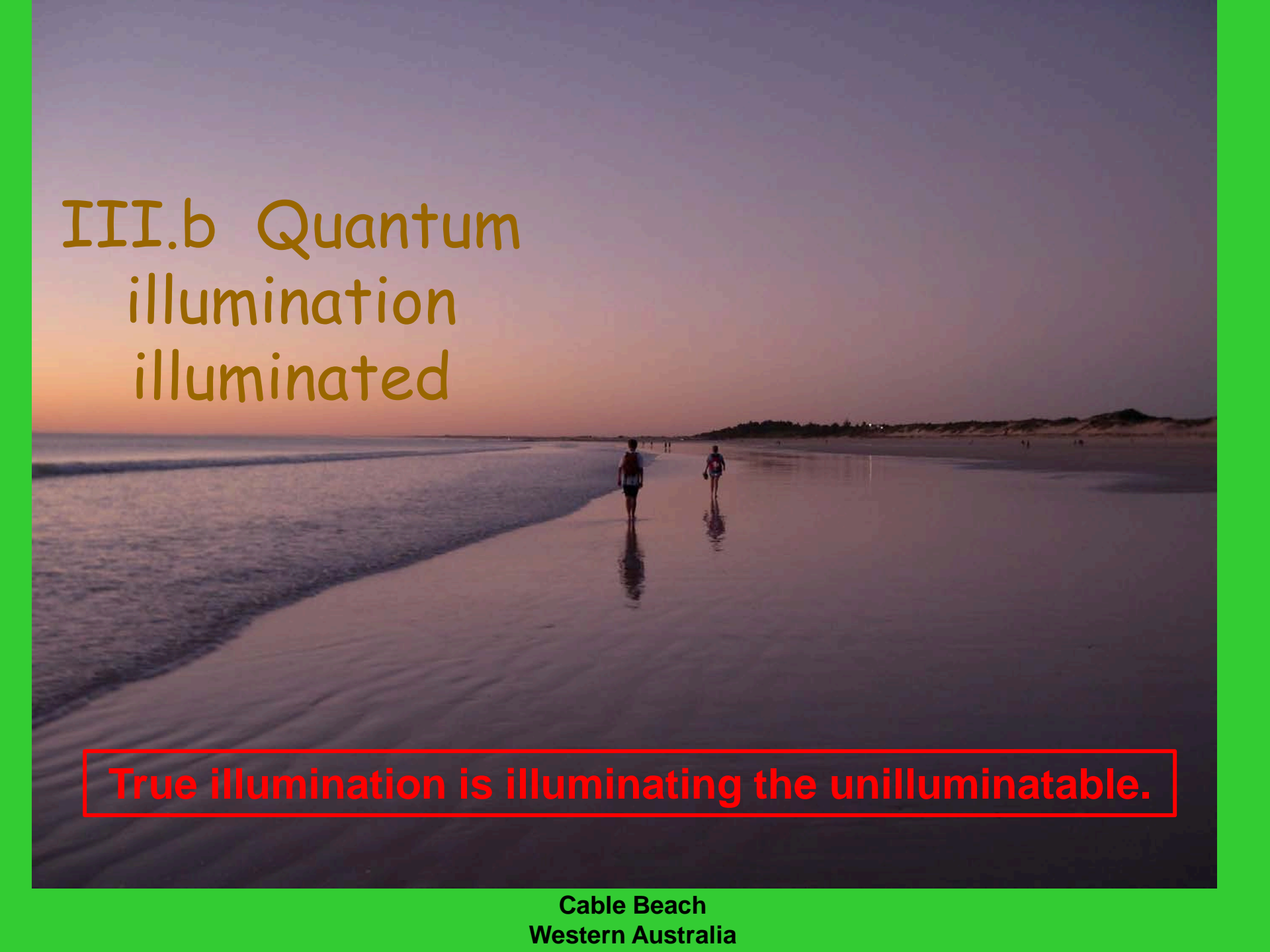


Randomized boson sampling runs

A. P. Lund, A. Laing, S. Rahimi-Keshari, T. Rudolph, J. L. O'Brien, and T. C. Ralph, PRL **113**, 100502 (2014).

Alice's single-photon counts produce a single photon into the corresponding inputs of Bob's pLON.



A photograph of Cable Beach at sunset. The sky is a mix of orange, pink, and blue. The ocean is calm with gentle waves. Two people are walking away from the camera on the wet sand, their figures reflected in the shallow water. The beach is wide and sandy, with some dunes visible in the distance.

III.b Quantum illumination illuminated

True illumination is illuminating the unilluminatable.

**Cable Beach
Western Australia**

Quantum illumination

R. Alexander and C. M. Caves, done, but paper not finished.

S. Lloyd, Science **321**, 1463 (2008)

S.-H. Tan, B. I. Erkmen, V. Giovannetti, S. Guha, S. Lloyd, L. Maccone, S. Pirandola, J. H. Shapiro, PRL **101**, 253601 (2008)

Problem: Detect a target against a background of thermal noise.

Problem: Distinguish no-target bath-idler state ($\theta = 0$),

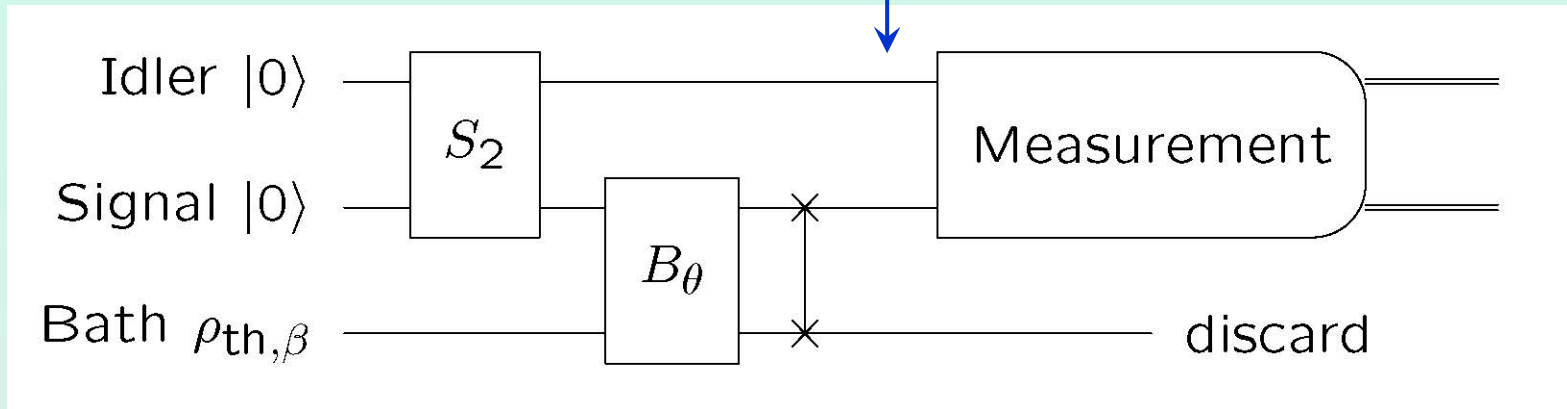
$$\rho_0 = \text{tr}_S(|r\rangle\langle r|) \otimes \rho_{\text{th},\beta} = \rho_{\text{th},\gamma} \otimes \rho_{\text{th},\beta},$$

($e^{-\gamma} = \tanh^2 r$) from target bath-idler state,

$$\rho_1 = \text{tr}_S(B_\theta |r\rangle\langle r| \otimes \rho_{\text{th},\beta} B_\theta^\dagger).$$

Two-mode squeezed state

$$|r\rangle = S_2|0,0\rangle = \frac{1}{\cosh r} \sum_{n=0}^{\infty} (-\tanh r)^n |n,n\rangle$$



Thermal state

$$\rho_{\text{th},\beta} = \frac{1}{Z_\beta} e^{-\beta \hat{a}_B^\dagger \hat{a}_B}$$

Beamsplitter

$$B_\theta = e^{-\theta(\hat{a}_S^\dagger \hat{a}_B - \hat{a}_S \hat{a}_B^\dagger)}$$

Crucial fact: $[n_B - n_I, \rho_1] = 0 \implies \rho_1$ (and ρ_0) is diagonal in sectors n spanned by number states $|\lambda, \lambda + n\rangle$; n is the difference in the number of bath and idler photons at the detector.

Quantum illumination

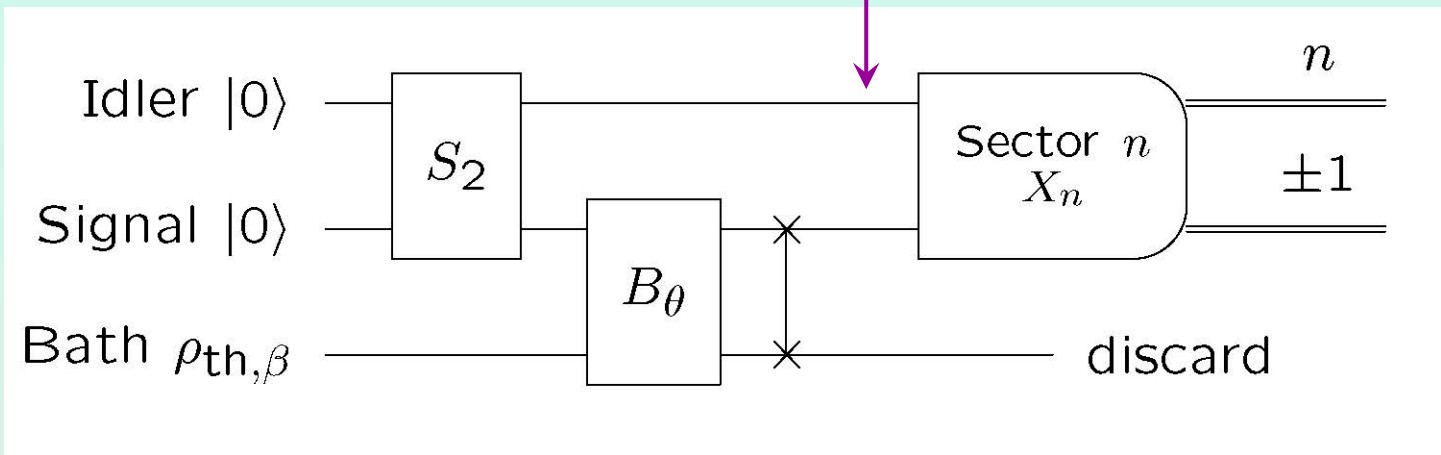
Problem: Detect a target against a background of thermal noise.

The regime of interest is a weak signal ($\theta \ll 1$) buried in high-temperature noise ($\beta \ll 1$), with weak squeezing ($r \ll 1$), in which case the sectors are qubits spanned by $|0_n\rangle = |0, n\rangle$ and $|1_n\rangle = |1, n+1\rangle$.

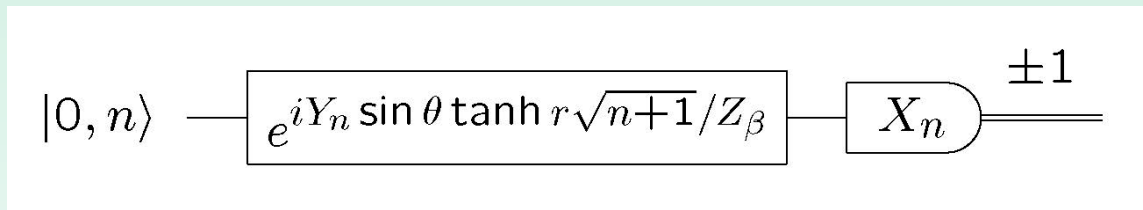
Pauli operators in qubit sectors

$$\begin{aligned} Z_n &= |0, n\rangle\langle 0, n| - |1, n+1\rangle\langle 1, n+1| \\ X_n &= |0, n\rangle\langle 1, n+1| + |1, n+1\rangle\langle 0, n| \\ Y_n &= -i|0, n\rangle\langle 1, n+1| + i|1, n+1\rangle\langle 0, n| \end{aligned}$$

$$\begin{aligned} \rho_0 &= |0\rangle\langle 0| \otimes \rho_{\text{th},\beta} \\ \rho_1 &= \frac{1}{Z_\beta} \sum_{n=0}^{\infty} e^{-\beta n} |\psi_n\rangle\langle \psi_n|, \quad |\psi_n\rangle = e^{iY_n \sin \theta \tanh r \sqrt{n+1} / Z_\beta} |0, n\rangle \end{aligned}$$



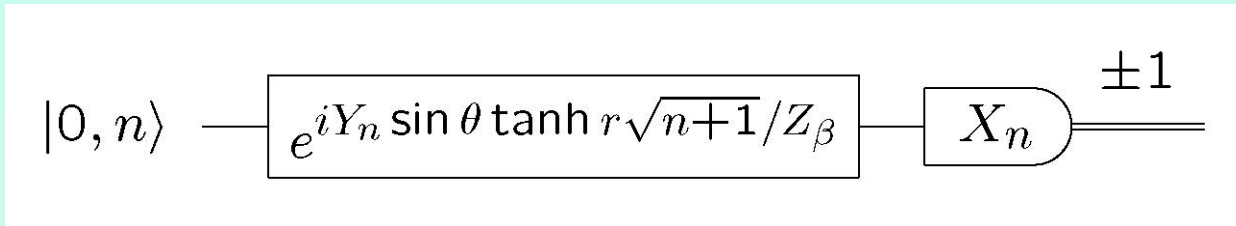
Qubit sector n : rotation about Bloch y axis



Quantum illumination

Problem: Detect a target against a background of thermal noise.

Qubit sector n : rotation about Bloch y axis



The probability of error in distinguishing ρ_1 from ρ_0 is an average over the qubit sectors:

$$P_e = \frac{1}{2} \left(1 - \frac{\sin \theta \tanh r}{Z_\beta} \sum_{n=0}^{\infty} \frac{e^{-\beta n}}{Z_\beta} \sqrt{n+1} \right) \simeq \frac{1}{2} \left(1 - \frac{1}{2} \sqrt{\frac{\pi}{Z_\beta}} \sin \theta \tanh r \right)$$

Previous work—and there is lots of it—did not recognize the sector structure, nor specialize to the weak-squeezing approximation, and so did not find the qubit structure and the Helstrom optimal measurement.

Quantum illumination: Role of entanglement

Problem: Detect a target against a background of thermal noise.

The signal-idler two-mode squeezed state $|r\rangle$ is entangled. The bath-idler state ρ_1 is separable, but each qubit sector is entangled.

So is entanglement important and, if so, how?

The point of the initial entanglement is to introduce correlations between the signal and idler, which survive, though barely, as entangled correlations between bath and idler in each qubit sector. Quantum illumination lives on the *coherence* between $|0, n\rangle$ and $|1, n + 1\rangle$ in each qubit sector, which is necessarily entanglement in the sector.

Quantum illumination: N-trial asymptotics

Problem: Detect a target against a background of thermal noise.

What I have said till now is not even close to the whole story. More important is the multi-trial asymptotics, where we have found the both the Helstrom error probability and the optimal measurement in the weak-squeezing approximation, and tight bounds on the error probability outside the weak-squeezing approximation.

This could be why it has taken forever to get our act together.

That's all, folks.
Thanks for your
attention.



Tent Rocks

Kasha-Katuwe National Monument, Northern New Mexico